

## REVIEW

# Imaging single molecules in living cells for systems biology

Yasushi Sako<sup>1,2,\*</sup>

<sup>1</sup> Cellular Informatics Laboratory, RIKEN, Wako, Japan and

<sup>2</sup> Formation of Soft Nanomachines, CREST, JST, Suita, Japan

\* Corresponding author. Laboratories of Nanobiology, Graduate School of Frontier Biosciences, Osaka University, 1-3 Yamadaoka, Suita 565-0871, Japan. Tel.: +81 6 6879 4426; Fax: +81 6 6879 4427; E-mail: sako@phys1.med.osaka-u.ac.jp

Received 21.7.06; accepted 6.9.06

**In this work, I present the application of single-molecule imaging to systems biology and discuss the relevant technical issues within this context. Imaging single molecules has made it possible to visualize individual molecules at work in living cells. This continuously improving technique allows the measurement of non-invasively quantitative parameters of intracellular reactions, such as the number of molecules, reaction rate constants and diffusion coefficients with spatial distributions and temporal fluctuations. This detailed information about unitary intracellular reactions is essential for constructing quantitative models of reaction networks that provide a systems-level understanding of the mechanisms by which various cellular behaviors are emerging.**

*Molecular Systems Biology* 17 October 2006;

doi:10.1038/msb4100100

**Subject Categories:** simulations and data analysis; signal transduction

**Keywords:** microscopy; protein–protein network; reaction dynamics; reaction kinetics

## Introduction

In 1995, purified biological molecules that had been conjugated with single fluorophores were first visualized as single molecules in aqueous conditions (Funatsu *et al.*, 1995). A few years later, two research groups succeeded in imaging single molecules in living cells (Sako *et al.*, 2000; Schütz *et al.*, 2000). Since this time, single-molecule imaging (SMI) has developed into one of the major techniques in biophysics to study structures, functions and the transition of the states of biomolecules.

In SMI in living cells, the molecules of interest are conjugated with fluorophores and introduced into cells. The behavior of multiple fluorescent molecules in cells is then visualized using high-sensitivity video microscopy. The observables in SMI are the position or movement of the fluorescent spots, the fluorescence intensity of individual

spots, the fluorescence spectrum or color of individual spots, and the number and distribution of the spots. Importantly, in SMI, the distributions and fluctuations of these parameters can be obtained in addition to the averages, which can be obtained in multiple-molecule experiments. These observables provide information about the structure of the molecules, the reaction parameters of the molecules, the transitions between molecular states, and the microenvironments and microstructures surrounding the molecules. For example, intra- and inter-molecular fluorescent resonance energy transfer (FRET) between single fluorophores (so-called ‘single-pair’ FRET) provides information on the molecular structure, whereas movements of single molecules may reflect the presence of microdomains in biomembranes or the cytoskeletal tracks. Because SMI is a non-invasive technique, it allows measurements of reactions under physiological conditions inside living cells.

In this work, I will focus on SMI as a technique that provides fundamental information on molecular systems. In systems biology, simulation of molecular networks invariably faces a particularly acute problem, which is the lack of quantitative information about unitary reactions. Thus, the concentrations of proteins, the kinetic parameters of protein–protein interactions and enzymatic reactions, and the dynamic parameters of molecules such as the diffusion coefficient are largely unknown for most of the reactions inside cells. SMI is one of the few methods that allows these parameters to be determined *in vivo*. Among the major advantages of SMI are that SMI achieves a quantitative analysis without destroying cellular integrity and provides information about the distribution and fluctuations of the parameters as well as the averages. Several practical aspects of data collection and analysis are also described here. General usage of SMI in living cells has been reviewed elsewhere (Sako and Yanagida, 2003; Wazawa and Ueda, 2005).

## Techniques of SMI in living cells

Because it is still difficult to perform SMI in intact tissues or whole organisms, this work will focus on applications in cultured cells.

### Microscopy

The most important technical issue to address in SMI is background rejection, although sensitivity is not a major concern for recent video camera systems. For this reason, the coverslips onto which cells are cultured should be thoroughly cleaned. Phenol red, which has slight fluorescence, should also be removed from the culture medium. Cells exhibit autofluorescence but usually it is not strong enough to obstruct the SMI signal except for highly fluorescent vesicles (of unknown identity) that occasionally appear in the vicinity of

the nucleus. Thus, the major sources of background are the fluorescence signals of molecules that are out of focus and the scattering and autofluorescence from dust in the specimen, optics and medium.

Total internal reflection (TIR) illumination and low-angle oblique (LAO) illumination are the main techniques for background rejection in SMI in living cells (Figure 1). Conventional epi-illumination can be applicable when the concentration of fluorophore is low and scattering in the specimen is small. However, TIR fluorescence microscopy has become the most popular technique for SMI. TIR is an optical phenomenon that occurs when the incident angle of the excitation light beam becomes greater than a critical value. Under these circumstances, the light is totally reflected at the coverslip–water interface. This reflection generates an electromagnetic field—the evanescent field—which decays exponentially along the depth into the water. TIR fluorescence microscopy uses this evanescent field, which has a typical decay length of about 200 nm, therefore avoiding the excitation of molecules that are out of focus. Although TIR illumination realizes extremely good contrast, its main use in cell biology is limited to observation near the basal cell surface. In order to observe deep inside cells, such as nuclear

pore complexes (Yang *et al*, 2004) or the apical membrane (Teramura *et al*, 2006), LAO illumination is applicable. LAO uses a thin light layer made by refracting a laser beam that has an incident angle that is slightly smaller than the critical angle of TIR. The contrast in LAO is not as good as TIR but far better than the epi-illumination. However, because LAO illuminates thick volumes of the cell, it cannot be used when fluorescent molecules are dense and widely dispersed three-dimensionally. The higher limit of the concentration of fluorophore in TIR illumination is about 100 nM. Above that concentration, more than one soluble fluorescent molecule will be present in the focal volume at the surface (200 nm in radius and 200 nm in height), which decreases the signal-to-background ratio to values that are less than one. In LAO illumination, the concentration should be less than 1 nM. TIR and LAO can be easily interchanged by altering the incident angle of the excitation laser beam.

The usual settings of commercial TIR (LAO) microscopes use one-sided laser illumination. In this setting, the interference patterns of laser sometimes destroy the image, and/or, owing to the concave shape of cells and anisotropic cellular structures, the image will not be good. These problems can be overcome by illumination from several directions using multiple beams or a circular laser beam (Figure 1C).

A spinning microlens array type of confocal microscope has been used for SMI of purified proteins on the glass surface (Tadakuma *et al*, 2001) and would in principle be applicable in living cells. Having a better lateral spatial resolution compared with TIR or epi-illumination, it would be well suited for dense samples.

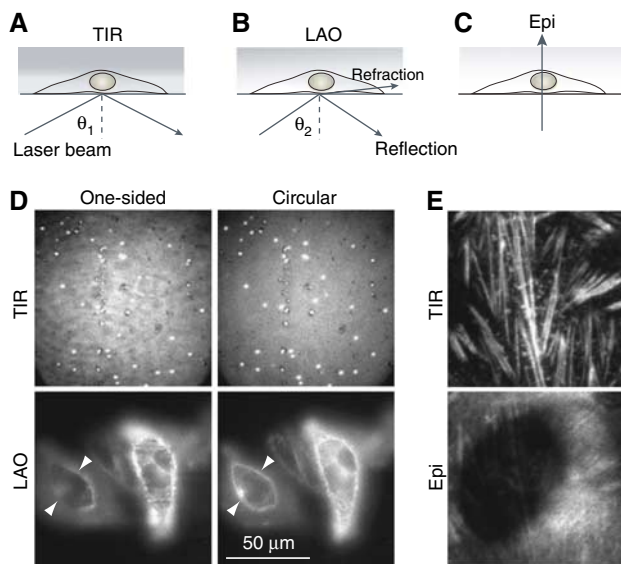


**Figure 1** Microscopy for SMI in living cells. **(A)** TIR illumination, in general, allows the basal membrane of cells to be visualized. **(B)** LAO illumination, in which entire cells can be illuminated, offers a better contrast as compared with conventional epi-illumination. The relationship between the incident angle in **A** ( $\theta_1$ ), **B** ( $\theta_2$ ) and the critical angle of TIR ( $\theta_c$ ) is  $\theta_1 > \theta_c > \theta_2$ . **(C)** Conventional epi-illumination. **(D)** Images of the same fields using one-sided (left panels) or circular (right panels) illumination in the TIR (fluorescent beads on the glass surface are covered with fluorophores; upper panels) or LAO mode (cells expressing a high density of membrane protein fused with GFP (lower panels). Interference patterns (in TIR), or smears and inhomogeneous illumination (in LAO) are obvious in one-sided illuminations. Circular illumination is realized by using a doughnut-shaped laser beam that is focused on the back focal plane of the objective. **(E)** A comparison between TIR and epi-illumination. The same field of a cell expressing GFP-actin was observed by focusing on the basal membrane. The dynamic range of the signal is adjusted between two images. Stress fibers on the basal membrane are clearly observed in TIR (upper panel) but are obscured in epi-illumination (lower panel) by the background from the cytoplasm and apical membrane. The dark circular region in the epi-image is the nucleus from which actin fibers are excluded.

## Technical limitations of SMI in living cells

There are three major limitations of SMI in living cells, which will hopefully be overcome in the near future. At present, these limitations should be taken into consideration when planning SMI experiments.

### Spatial resolution

Spatial resolutions of optical microscopy are usually limited to 100–200 nm in the focal plane. This limitation governs the upper limits of the density of membrane particles and soluble molecules to be about  $10 \mu\text{m}^{-2}$  and 100 nM, respectively, even when TIR illumination is used. Techniques using nanofabrication of the observation chamber that is smaller than the wavelength of light (zero-mode waveguides) have been proposed to overcome this limitation for *in vitro* SMI measurements. But these techniques are difficult to apply to living cells. Micrometer-scale structures and movements of molecules in cells cannot be observed using this technique. Because single-pair FRET is detectable in living cells (Sako *et al*, 2000), this technique might be applied in order to detect nanometer-scale molecular interactions.

### Photostabilities of the fluorophores

The typical number of images that can be taken from single molecules before photobleaching is in the order of 300–1000 (<30 s in 30 frames/s of video rate). Antioxidants

are widely used in *in vitro* SMI experiments to prevent photobleaching but are problematic in *in vivo* experiments because eliminating oxygen will reduce the viability of cells. Tetramethylrhodamine (TMR), Cy3, Cy5 and Alexa 488 can be used for SMI in living cells. Many species of chemical fluorophore that are reactive to amino-terminal lysine, cysteine and glutamate residues in proteins can be obtained. The labeled proteins need to be introduced into cells using microinjection, bead loading, electroporation or other techniques. Green fluorescent protein (GFP) and yellow fluorescent protein (YFP) have also been successfully used. GFP and related gene expression technologies are convenient for fluorescent labeling of molecules inside cells. However, GFP and its variants are readily photobleached and blinking is noticeable especially for YFP. In practice, I recommend the use of TMR or Cy3 as first-choice fluorophores. When fluorescent proteins have to be used, enhanced green fluorescent protein seems to be the best. Quantum dots can be visualized in single particles with a strong fluorescent signal and extremely long observation period (>1 min at video rate) before photobleaching. However, owing to prominent blinking, difficulty in chemistry for stoichiometric labeling and steric hindrance, the application of quantum dot in SMI to detect kinetic and dynamic properties of reactions is limited. Of course, after labeling with fluorophores, the biological activities of the labeled molecules have to be confirmed using conventional biochemical and cell biology assays.

### Software for image processing

There is as yet no standard algorithm for processing SMI data. Especially in living cells, owing to inhomogeneous backgrounds in both space and time, the automatic detection of single-molecule spots and the calculation of their positions and fluorescence intensities are difficult. In our laboratory, the image profiles at a single molecule are usually fit to a two-dimensional Gaussian distribution on an inclined plane. The center and the integral of the Gaussian distribution represent, respectively, the position and the fluorescence intensity of the spots. To track the movements of spots, the nearest spot in the next video frame is thought to be the same one in the previous frame. However, the results of automatic calculation need to be verified by directly looking at the movies with care.

## Applications of SMI in systems biology

### Counting numbers of molecules involved in cellular reactions

There is limited information on the concentrations and numbers of molecules involved in intracellular reactions even though these parameters are important to understanding molecular systems. The quantitative nature of SMI allows the number of molecules to be counted. Using SMI in conjunction with observations of cell morphology or cellular responses, it has been found that the number of extracellular signaling molecules required to induce some cellular responses can be very small. For example, chemotaxis of *Dictyostelium discoideum* cells could be induced by 400 molecules of cyclic AMP

(cAMP) per cell (Ueda *et al.*, 2001) and the extension of the growth cone of chick dorsal root ganglion cells was triggered by only 40 molecules of nerve growth factor per single growth cone (Tani *et al.*, 2005). In HeLa cells, 300 molecules of epidermal growth factor (EGF) were enough to induce an intracellular calcium response (Uyemura *et al.*, 2005). In the case of cAMP gradient sensing by *D. discoideum*, the difference in the numbers of cAMP molecules along the gradient could be less than 10 (Ueda *et al.*, 2001). Therefore, fluctuations that are due to finite-number effects are not negligible in intracellular systems. To prevent the activation of inappropriate responses, cells therefore need to be able to distinguish small signals from large noise. The sigmoidal response curves and feedback regulation motifs that are found in various intracellular pathways are thought to be important for noise reduction. It is however also possible that cells sometimes make use of the noise to improve sensitivity to signals, as shown in the case of stochastic resonance.

### Kinetic analysis in living cells

The kinetic analysis of reactions in living cells is problematic when applied at the multiple-molecule level. Measuring reaction rate constants under these conditions requires the synchronization of the individual reactions. However, synchronization is often impossible in complicated molecular networks. In addition, step changes in concentration or temperature, which are usually applied to achieve synchronization, change the condition of the system. Therefore, it is difficult to analyze reactions at a quasi-steady state in multiple-molecule experiments.

Because SMI allows multiple individual reactions to be observed and recorded simultaneously, measurements of rate constants can be achieved without synchronization. The starting points of each reaction can then be identified *a posteriori* and set to time zero for statistical analysis of the ensemble. Such *in vivo* SMI measurements at quasi-steady state have revealed spatial inhomogeneity of the reaction parameters (Ueda *et al.*, 2001; Watanabe and Mitchison, 2002). To measure dissociation rates, the binding durations (on-time) of single events of association are determined by SMI (Figure 2A), and the rate constants are calculated from the decay of the histogram of on-times using a similar reaction rate equation as in multiple-molecule analysis (Xie, 2001; see Supplementary information for details). Similarly, by measuring the periods from the detachment of a molecule to the attachment of the next molecule (off-time), the association rate constant can be deduced. However, in this case, single binding sites must be monitored during at least two consecutive association events; otherwise, a synchronization of the reactions is required (Tani *et al.*, 2005). If association–dissociation cycles can be observed on the same single binding site, one can even determine the reaction rate for individual binding sites to assess static (site-to-site) and dynamic (temporal) fluctuations in the reaction (Xie, 2001).

### Combination of SMI and mathematical modeling

SMI provides quantitative information of the unitary reactions inside cells that is otherwise difficult to obtain using

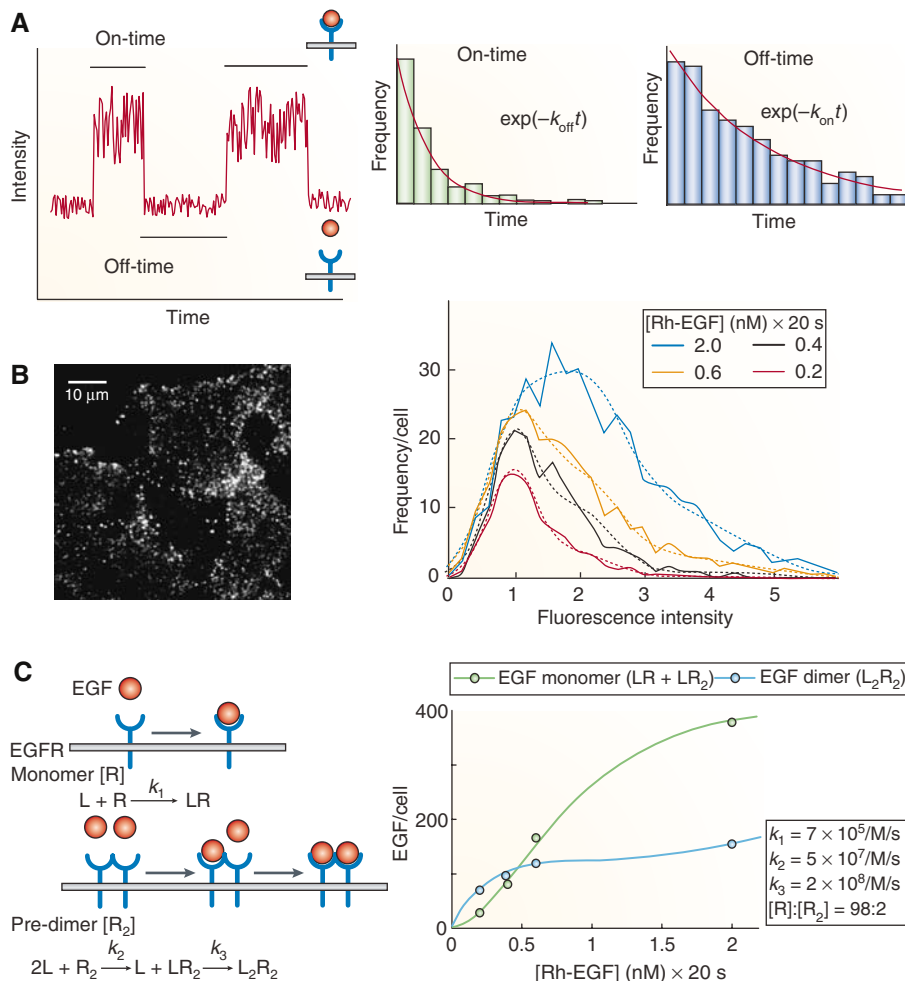


**Figure 2** Single-molecule kinetics in living cells. **(A)** Association and dissociation rate constants can be determined by statistical analysis of the single-molecule off-time and on-time measurements, respectively. The cartoon shows a simple two-state reaction. **(B)** Cluster size distribution can be determined from a histogram of single-molecule spot intensities. Here, cells were incubated with various concentrations of fluorescent EGF (TMR-EGF) for 20 s (left). The distributions (right) were fitted by the sum of four Gaussian functions (dashed lines). Gaussian distribution of the fluorescence intensity was confirmed from the single-molecule fluorescence intensity distribution of TMR-EGF on the glass surface. The fluorescence intensity was normalized with respect to that of a single molecule. **(C)** Using data from panel B and reaction models (left), the association rate constants between EGF and its receptor, and the ratio between receptor monomers and pre-dimers have been determined (right). In this case, the receptors are known to form monomers and pre-dimers. The total number of receptor per cell is also known to be  $5.5 \times 10^4/\text{cell}$  (Berkers *et al*, 1991). See Supplementary information for details of the analysis.

conventional techniques. Such information can be used for determining pathways and/or predicting the dynamic behaviors of reaction networks. Determining the kinetic parameters for the rate-limiting steps of the reaction network is particularly relevant.

In this section, a simple example is presented on how to analyze the process of EGF association with its receptor (EGFR) using SMI and mathematical modeling (Uyemura *et al*, 2005). EGFR, a membrane receptor that is responsible for cell proliferation, is known to form dimers and larger clusters at the cell surface. In particular, the formation of EGFR dimers with two bound EGF molecules is known to be indispensable for activating EGFR signaling.

In SMI analysis, the cluster size of the bound ligand conjugated with a fluorophore can be determined from the fluorescence intensity (Figure 2B). Detecting the cluster size distribution is another advantage of SMI (Nguyen *et al*, 2006).

The distribution of the fluorescence spot intensity can be fitted with a sum of the Gaussian functions to obtain the distribution of cluster size. In the fitting, the peaks of the functions are set to multiples of the single-molecule intensity, as determined from the photobleaching step size. Single fluorescent molecules are photobleached in a single step, while the fluorescence intensity of a spot that contains many numbers of fluorophores gradually decays by photobleaching. It is likely that the single-step disappearance of fluorescent spots is caused by dissociation events rather than photobleaching. Dissociation and photobleaching can be distinguished by changing the excitation intensity, as dissociation kinetics does not depend on the excitation intensity. The standard deviations of the Gaussian functions to fit the fluorescence intensity histograms are proportional to the square of the number of molecules contained in each peak when fluctuation of the photon count represents the main



source of noise (stochastic processes, such as fluorescence emission, are indeed characterized by their variability being proportional to the square of the mean). If self-quenching takes place between molecules at a single binding site, the spot intensities will not be proportional to the number of molecules at the site. This can be determined by comparing the step sizes of the last and the second-last photobleaching at spots that contain multiple molecules. Owing to limitations in the spatial resolution, it is possible that molecules that are not bound to the same binding site but are in close proximity form single spots. In this case, the synchronized movement of two molecules represents strong evidence for real clustering (Teramura *et al.*, 2006). Figure 2B shows the result of the cluster size distribution analysis of EGF conjugated with TMR (TMR-EGF) bound to EGFR. The distribution depends on the concentration of TMR-EGF applied to cells.

In the example shown in Figure 2C, the cluster size distributions of TMR-EGF are used to estimate the association rate constants between EGF and EGFR (Figure 2C; also see Supplementary information for details). The model for the association reactions between EGF and EGFR monomers and dimers is depicted in Figure 2C (left). In this model, trimers and tetramers are considered to be combinations of monomers and dimers for simplification. The association reactions are then modeled by coupled differential equations, which can be solved to derive expressions of the amount of each species as a function of time and ligand concentration (see Supplementary information). These functions are then fitted to two experimental data sets that describe the ligand densities—which is the labeled species in this particular example—bound as monomers or dimers as a function of the concentration of the ligand applied. The resulting best-fit parameters suggest a larger association rate to receptor dimers than to monomers ( $k_1 < k_2$ ) and a positive cooperativity in ligand binding to the receptor dimers ( $k_2 < k_3$ ). These characteristics were not known previously and are thought to be important for effective dimerization and activation of EGFR at low concentrations of EGF. This technique has now been extended to a reaction network that contains six unit reactions and two initial concentrations and has been successful in determining reaction pathways and parameters for the formation of signaling dimers of EGFR (Teramura *et al.*, 2006). In this study, the positive cooperativity predicted by Uyemura *et al.* (2005) is confirmed and it is suggested that it depends on an allosteric conformational change of EGFR dimers.

### Single-molecule dynamics

Another popular usage of SMI in living cells at the present time is for detecting the dynamic properties of molecules, including lateral diffusion coefficients and the velocities of vectorial transport of membrane components (Schütz *et al.*, 2000; Tani *et al.*, 2005; Shibata *et al.*, 2006; Figure 3). The movements of membrane components also provide information about local microstructures of cells such as membrane microdomains (Douglass and Vale, 2005). Techniques of single-particle tracking are also available for this purpose (Saxton and Jacobson, 1997). However, in spite of the limitations in the observation period due to photobleaching and in positional accuracy due to the low signal-to-noise ratio, SMI is superior

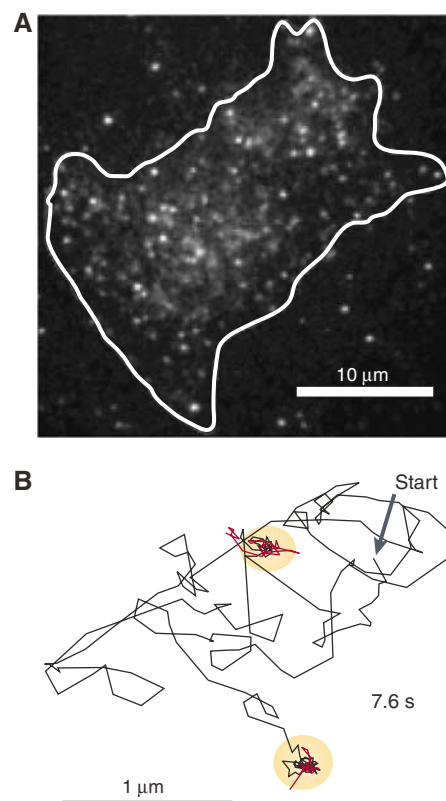


**Figure 3** Single-molecule tracking in living cells. **(A)** Cy3-NGF (nerve growth factor) bound to the surface of a PC12 cell. The white line delineates the shape of the cell. **(B)** Single-molecule trajectories of the receptor–ligand (Cy3-NGF) complex on the cell surface. The movement of the complex displayed repeated alternation between mobile and immobile phases. During immobile phases (yellow circles), the complex formed clusters with other complexes (red trajectories).

for stoichiometric analysis and avoids steric problems, compared with single-particle tracking, which uses much larger probes.

Quantitative modeling and simulation of biological networks in systems biology will have to be extended to include both static and dynamic spatial inhomogeneities in the reaction systems. Indeed, most of the protein–protein interactions in living cells, at least in principle, should be understood as reaction–diffusion systems. Diffusion terms are expected to be significant, especially in reactions occurring at the biomembrane, which has high a viscosity, but also in the crowded and dense intracellular environments. In fact, correlations between the movements and reactions of membrane proteins have been reported (Murakoshi *et al.*, 2004; Shibata *et al.*, 2006). Combinations of kinetic and dynamic analysis in SMI should be extended in the future to achieve a quantitative understanding of the mechanisms that underlie polarization and movements of cells, as diffusion terms are thought to determine the output of the reaction networks that control these biological processes.

### Conclusion and perspectives

SMI has made it possible to observe the behavior of individual biomolecules at work in living cells. Compared with multiple-

molecule techniques, SMI is superior in its quantitative nature. Therefore, combinations of SMI and mathematical modeling will be powerful in systems biology. On the one hand, SMI can provide reaction parameters that are essential for mathematical modeling. On the other hand, detailed prediction made by quantitative modeling of reactions can be validated using SMI. Intracellular reaction networks are extremely complex and it may be impossible to measure all of the unitary reactions in single molecules. However, using SMI at key steps of the reaction networks will provide novel insights and reliable quantitative information for systems biology. Techniques for SMI in living cells are continuously improving and it should be possible, in the near future, to develop automated SMI for diagnosis and drug-screening purposes. From the point of view of the fundamental insights provided by this technique, single-molecule experiments are uncovering large fluctuations in the structure and reaction parameters of biomolecules. Furthermore, SMI reveals that the number of molecules involved in cellular reactions is small, which has consequences for large fluctuations. Hence, one of the next major challenges in systems biology will be to incorporate such fluctuations into reaction network models to reveal how biological networks produce flexible cellular behaviors.

## Supplementary information

Supplementary information is available at the *Molecular Systems Biology* website ([www.nature.com/msb](http://www.nature.com/msb)).

## References

- Berkers JAM, Van Berger en Henegouwen PMP, Boonstra J (1991) Three classes of epidermal growth factor receptors on HeLa cells. *J Biol Chem* **266**: 922–927
- Douglass AD, Vale RD (2005) Single-molecule microscopy reveals plasma membrane micro domains created by protein–protein networks that exclude or trap signaling molecules in T cells. *Cell* **121**: 937–950
- Funatsu T, Harada Y, Tokunaga M, Saito K, Yanagida T (1995) Imaging of single fluorescent molecules and individual ATP turnover by single myosin molecules in aqueous solution. *Nature* **374**: 555–559
- Murakoshi H, Iino R, Kobayashi T, Fujiwara T, Ohshima C, Yoshimura A, Kusumi A (2004) Single-molecule imaging analysis of Ras activation in living cells. *Proc Natl Acad Sci USA* **101**: 7317–7322
- Nguyen AH, Nguyen VT, Kamio Y, Higuchi H (2006) Single-molecule visualization of environment-sensitive fluorophores inserted into cell membranes by staphylococcal  $\gamma$ -homolysin. *Biochemistry* **45**: 2570–2576
- Sako Y, Minoguchi S, Yanagida T (2000) Single molecule imaging of EGFR signal transduction on the living cell surface. *Nat Cell Biol* **2**: 168–172
- Sako Y, Yanagida T (2003) Single-molecule visualization in cell biology. *Nat Rev Mol Cell Biol* **4** (Suppl): SS1–SS5
- Saxton MJ, Jacobson K (1997) Single-particle tracking: applications to membrane dynamics. *Annu Rev Biophys Biomol Struct* **26**: 373–399
- Schütz GJ, Gerald K, Pastuchenko VP, Schindler H (2000) Properties of lipid microdomains in a muscle cell membrane visualized by single molecule microscopy. *EMBO J* **19**: 892–901
- Shibata SC, Hibino K, Mashimo T, Yanagida T, Sako Y (2006) Formation of signal transduction complexes during immobile phase of NGFR movements. *Biochem Biophys Res Commun* **342**: 316–322
- Tadakuma H, Yamaguchi J, Ishihama Y, Funatsu T (2001) Imaging of single fluorescent molecules using video-rate confocal microscopy. *Biochem Biophys Res Commun* **287**: 323–327
- Tani T, Miyamoto Y, Fujimori K, Taguchi T, Yanagida T, Sako Y, Harada Y (2005) Trafficking of ligand–receptor complex on the growth cones as an essential step for the uptake of nerve growth factor at the distal end of the axon: a single-molecule analysis. *J Neurosci* **25**: 2181–2191
- Teramura Y, Ichinose J, Takagi H, Nishida K, Yanagida T, Sako Y (2006) Single-molecule analysis of epidermal growth factor binding on the surface of living cells. *EMBO J* **25**: 4215–4222
- Ueda M, Sako Y, Tanaka T, Devreotes P, Yanagida T (2001) Single-molecule analysis of chemotactic signaling in *Dictyostelium* cells. *Science* **294**: 864–867
- Uyemura T, Takagi H, Yanagida T, Sako Y (2005) Single-molecule analysis of epidermal growth factor signaling that leads to ultrasensitive calcium response. *Biophys J* **88**: 3720–3730
- Watanabe N, Mitchison TJ (2002) Single-molecule speckle analysis of actin filament turnover in lamellipodia. *Science* **295**: 1083–1086
- Wazawa T, Ueda M (2005) Total internal reflection fluorescence microscopy in single molecule nanobioscience. *Adv Biochem Eng Biotechnol* **95**: 77–106
- Xie S (2001) Single-molecule approach to enzymology. *Single Mol* **2**: 229–236
- Yang W, Gelles J, Musser SM (2004) Imaging of single-molecule translocation through nuclear pore complexes. *Proc Natl Acad Sci USA* **101**: 12887–12892